Solar Neutrinos

Yoichiro Suzuki
Kamioka Observatory
Institute for Cosmic Ray Research
University of Tokyo
Higashi-Mozumi, Kamioka
Gifu 506-1205, Japan

1 Introduction

We now recognize that neutrinos have finite masses. In 1998, the Super-Kamiokande experiment found evidence for the atmospheric neutrino oscillation [1]. The significance of the observation is very strong: $\Delta\chi^2 = 120$ between the no oscillation hypothesis and the best-fit parameter set. The data also supports the $\nu_\mu \rightarrow \nu_\tau$ mode for the atmospheric neutrino oscillation at the 99% confidence level.

The next important issue to be resolved towards the full understanding of the neutrino oscillation phenomena is the so-called solar neutrino problem. This is most likely an oscillation of the $\nu_e \rightarrow \nu_\mu$ mode, which is more or less de-coupled from the atmospheric neutrino oscillation.

The solar neutrino problem has been present since early 1970 [2], well before the first indication of the atmospheric neutrino anomaly by Kamiokande in 1988 [3]. The problem has remained for nearly 30 years without a complete solution (in the sense that we have not reached to the unique oscillation parameters). However, the indication of the neutrino oscillation is getting stronger as time evolves.

Here we summarize the present situation of the solar neutrino problem, mostly from the experimental point of view, and briefly express the perspective for the near future.

2 Solar neutrino spectrum

Solar neutrinos are produced by nuclear reaction chains in the central core of the sun. The solar neutrino flux depends upon the core temperature of the sun, its chemical composition, the cross sections of the nuclear reactions, the opacity of the sun, and so on. The largest fraction of the solar neutrinos are produced by the

so called pp-chain; a smaller fraction (1.6 %) is believed to be produced through the CNO cycle. In the pp-chain, the following five nuclear reactions produce neutrinos:

$$\begin{aligned}
p + p &\rightarrow d + e^+ + \nu_e \qquad (E_\nu < 0.42 \text{ MeV}) \\
p + e + p &\rightarrow d + \nu_e \qquad (E_\nu = 1.44 \text{ MeV}) \\
e + {}^7\text{Be} &\rightarrow {}^7\text{Li} + \nu_e \qquad (E_\nu = 0.86 \text{ MeV (90\%)},\ 0.38 \text{ MeV (10\%)}) \\
{}^8\text{B} &\rightarrow {}^8\text{Be}^* + e^+ + \nu_e \qquad (E_\nu < 15 \text{ MeV}) \\
{}^3\text{He} + p &\rightarrow {}^4\text{He} + e^+ + \nu_e \qquad (E_\nu < 18.8 \text{ MeV})
\end{aligned}$$

The corresponding neutrinos are called pp-, pep-, ^{7}Be-, ^{8}B-, and hep-neutrinos respectively. Most of the solar neutrinos ($\sim$ 91%) are produced by the pp fusion reactions (pp-neutrinos). The ^{7}Be-neutrinos are monochromatic and give about 10% of the pp-neutrino flux. The high-energy ^{8}B-neutrinos (with an end point energy of 15 MeV) contribute a small fraction (0.008%) of the total flux. The highest energy neutrinos are the hep-neutrinos, with an end point energy of 18.8 MeV. However, their flux is about three orders of magnitudes smaller than the ^{8}B-neutrino flux.

The solar neutrino spectrum is well calculated by standard solar models (SSMs) [4, 5]. The results of the BP98 SSM [4]are shown in Fig. 1. The BP98 model uses newly reevaluated nuclear reaction rates [6], the 1996 Livermore OPAL opacities [7], the OPAL equation of state [8], and screening effects indicated in recent calculations [9]. The resultant changes from the BP95 SSM [10] are that: 1) the ^{8}B flux is reduced to $5.15 \times 10^6 \text{cm}^{-2}\text{s}^{-1}$ (from 6.14 for BP95), 2) the Cl capture rate is reduced to $7.7^{+1.2}_{-1.0}$ SNU (from 9.3 for BP95) 3) the Ga capture rate is reduced to 129^{+8}_{-6} SNU (from 137 for B95).

The net effect of the fusion reactions is

$$4p \rightarrow {}^4He + 2e^+ + 2\nu_e + 26.731 \text{ MeV}.$$

If we assume equilibrium in the sun, the energy released in the fusion reactions is related to the total flux of the solar neutrinos. The solar luminosity is determined by that energy, with a small correction for the energy carried away as kinetic energy of neutrinos and ions. Therefore, the solar luminosity constrains the solar neutrino fluxes [11, 12].

The recent development of helioseismology supports the validity of the standard solar models, taking into account helium and heavy element diffusion [13, 14]. Helioseismology determines the sound velocity in the sun with the typical accuracy of less than $\pm$0.1%, using thousands of measurements of the solar frequencies (p-mode) with an accuracy of $\Delta\nu/\nu$=10^{-4}. The standard model predictions of the radius, the radiation/convection boundary, R_b=0.714 $R_\odot$, and the

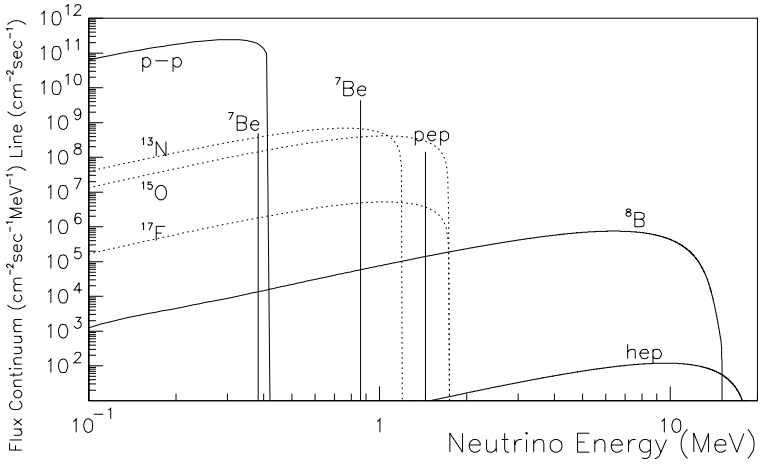

Figure 1: The solar neutrino spectrum calculated by the BP98 standard solar model [4]. Several tens of billions of solar neutrinos traverse a square cm of the earth each second.

density at that point, ρ_b=0.186 g/cm^3, agree with those determined by helioseismology, R_b=0.711(1±0.4%)R_o and ρ_b=0.192(1±0.4%)g/cm^3. The sound velocity in the sun also agrees to better than 0.2% at most depths. The most impressive recent development is that the sound velocity agrees to better than 1% even in the center of the core, $R < 0.1\ R_\odot$. The ^{8}B-neutrinos and ^{7}Be-neutrinos are produced at the typical depth of 0.04 $R_\odot$ and 0.06 $R_\odot$, respectively. Therefore, we now have evidence that the standard solar model is approximately correct even at the place where the neutrinos are produced.

The solar neutrino flux uncertainties, then, come mostly from nuclear physics uncertainties [6]. At the energy where solar fusion reactions takes place (5 to 30 keV), the Coulomb repulsion barrier is important. Therefore, the cross sections for the nuclear reactions in the sun are usually written by using a so called astronomical S-factor, S(E):

$$\sigma(E) = \frac{S(E)}{E} \exp\{-2\pi\eta(E)\} ,$$

where $\eta(E)$ is the Sommerfeld parameter and E is the center of mass energy. The exponential takes account of the tunneling through the Coulomb barrier. In order to obtain $\sigma(E)$ at $E \sim 0$ in the core of the sun, the $S(E)$ measured in the laboratory, typically at 0.1 to a few hundred MeV, must be extrapolated downward and a correction for the different screening effect between the laboratory and the sun must be taken into account. The uncertainty of the above procedures may not be well determined (see [6] for a detailed discussions). Note also that the laboratory experiments themselves sometimes have large systematic errors.

The uncertainty of $^{+19}_{-14}$% for the ^{8}B-neutrino flux comes mostly from the uncertainty of $S(0)$ for the production reaction $p + ^7\text{Be} \rightarrow ^8\text{B} + \gamma$. We do not have a reasonable way to determine the error for the hep-neutrino flux, associated with $S(0)_{hep}$. The importance of the hep-neutrinos near the end point energy of the ^{8}B spectrum has been pointed out recently; the accurate knowledge of the cross section of hep-neutrinos is very important [15, 16]. The uncertainty for the ^{7}Be-neutrinos is smaller than that for ^{8}B-neutrinos, about ± 7%, and the flux of pp-neutrinos are accurately determined to the level of 1%.

Another factor to be taken into account is the different temperature-dependence of each reaction. The ^{8}B-neutrinos depend on T as T_c^{25}, where T_c is the characteristic central temperature [17]. The ^{7}Be-neutrinos vary as T_c^{11}. The pp-neutrinos are relatively less dependent on the central temperature.

3 Solar neutrino experiments

The pioneering experiment on solar neutrinos was the Homestake Chlorine experiment [18], which started to take data in late 1960. This experiment has indicated the so-called 'solar neutrino problem', that the observed neutrino flux is smaller than the flux calculated from the SSMs.

Five solar neutrino experiments—Kamiokande [19, 20, 21], SAGE [22], GALLEX [23], Super-Kamiokande [24, 25, 26], and SNO [27, 28]—have been conducted since the time of the Homestake experiment. These experiments have used four different techniques (target materials) and therefore have different energy thresholds—233 keV for the Gallium experiments (SAGE and GALLEX), 814 keV for the Chlorine experiment (Homestake) and a few MeV for the water Cherenkov experiments (Kamiokande and Super-Kamiokande; 5.5 MeV for the latest analysis threshold of Super-Kamiokande), and, we expect, 5 MeV for the heavy water Cherenkov experiment (SNO). It is an advantage that these experiments have different energy thresholds and therefore have sensitivity to different regions of the solar neutrino spectrum.

The Chlorine and Gallium experiments are radio-chemical experiments. These measure the total integrated number of neutrino events above the particular threshold, accumulated for a month to a few months and sensitive only to the charged current interactions.

The Chlorine experiment utilizes the reaction:

$$\nu_e + ^{37}\text{Cl} \rightarrow e^- + ^{37}\text{Ar} \qquad (E_{th} = 814 \text{ keV}).$$

The SSM predicts a capture rate of 5.9 SNU for ^{8}B, 1.15 SNU for ^{7}Be, and 0.65 SNU for other neutrinos (pep-neutrinos and neutrinos from CNO cycle), where 1 SNU

(Solar Neutrino Unit) corresponds to 10^{-36} captures/atom/sec. The detector consists of 615 tons of C_2Cl_4. The produced-Ar-atoms are extracted by bubbling helium gas every two to three months. Auger electrons from the extracted Ar atoms are counted in small low background proportional counters. The result of the flux measurement of the Homestake experiment has persistently been about 30% of the SSM prediction. The most recent value reported is 2.56±0.16±0.16 SNU (data/SSM$_{BP98}$ = 0.332±0.021±0.021) [29].

The SAGE and GALLEX experiments (started in 1990 and 1991, respectively) use Ga as a target and are thus able to measure the lowest energy solar neutrinos. The predicted rates are 69.6 SNU from pp-neutrinos, through the reaction

$$\nu_e + {}^{71}\mathrm{Ga} \rightarrow e^- + {}^{71}\mathrm{Ge} \qquad (E_{th} = 233 \text{ keV}) \ ,$$

34.4 SNU from ^{7}Be-neutrinos, 12.4 SNU from ^{8}B-neutrinos, and 12.5 SNU from other sources.

The two experiments have provided consistent results. The flux observed by SAGE [22, 30] is $66.7^{+7.1}_{-6.8}$(stat.)$^{+5.4}_{-5.7}$(syst.) SNU. This corresponds to data/SSM$_{BP98}$ = $0.517^{+0.055}_{-0.053}$(stat.)$^{+0.042}_{-0.044}$(syst.). The result of GALLEX [23, 31] is $77.5^{+7.6}_{-7.8}$ SNU, corresponding to data/SSM$_{BP98}$ = $0.601^{+0.059}_{-0.060}$, with statistical and systematic errors combined in quadrature.

SAGE and GALLEX have performed measurements with artificial neutrino sources using ^{51}Cr [32] ($e^- + {}^{51}\mathrm{Cr} \rightarrow {}^{51}\mathrm{V} + \nu$), which provides mono-energetic neutrinos of 746 keV (81%), 751 keV (9%), 426 keV (9%) and 431 keV (1%). The GALLEX collaboration performed two such experiments, between September and December 1994, and between October and February 1996. The first experiment used 1.69±0.03 MCi of the ^{51}Cr source and gave a ratio of measurement to prediction of 1.01±0.10. The second used 1.86±0.02 MCi and showed the ratio to be 0.84±0.11 [33, 34]. The combined result is 0.93±0.08. SAGE has observed the ratio to be 0.95±0.12 [35]. These experiments demonstrate that the overall efficiency estimates of the gallium experiments are correct within ∼ 10%. Though calibration by the artificial neutrinos is in principle the best method, it is limited by the statistics. The GALLEX collaboration has added to their sample carrier-free ^{71}As, which decays with 2.72 days half-life to ^{71}Ge [36]. The ^{71}Ge produced in the target can be used to test the recovery efficiency of the experiment, which is proved to be better than 99%.

Kamiokande, Super-Kamiokande, and SNO are real-time electronic experiments using water Cherenkov technologies. The first two of these use pure water, while SNO uses heavy water (D_2O). All three are able to measure the event-time and energy. Directional information can be obtained from the ν_e+e interaction. The heavy water experiment can separately measure the neutral current contribution. We will discuss SNO later in this report.

The Kamiokande experiment, which showed the first evidence that neutrinos are actually coming from the sun's direction, terminated its solar neutrino observation on 6 February 1995. The final result [21] for the ^{8}B-solar neutrino flux, is $2.80\pm0.19(\text{stat.})\pm0.33(\text{syst.})\times10^6/\text{cm}^2/\text{s}$, based on the data taken from 2079 days of effective live time. This corresponds to data/SSM$_{BP98}$ = $0.544 \pm 0.037 \pm 0.064$ ($0.424 \pm 0.029 \pm 0.050$ for BP95 [10]).

Kamiokande showed that there was no evidence of time variation in accordance with solar activity within its experimental sensitivity. They also saw that there are no significant seasonal variations and day/night flux differences [20, 21]. Note, however, that the results on the time variation are limited by statistical and systematic uncertainties. A time variation smaller than the experimental sensitivities of Kamiokande is obviously not excluded.

Super-Kamiokande started to take data in 1996. It is a 50,000 ton water Cherenkov detector located 1000 m underground near the location of the Kamiokande detector. The present data is based on the effective 825 days of data between May 31, 1996, and April 3, 1999. The first 301 days are analyzed using a 6.5 MeV threshold, and the last 524 days are analyzed using a 5.5 MeV threshold [24]. The data below 6.5 MeV was only used for evaluating the energy spectrum. The number of events above 6.5 MeV is $11{,}235^{+180}_{-166}(\text{stat.})^{+315}_{-303}(\text{syst.})$. The total ^{8}B-neutrino flux, assuming the ^{8}B spectrum shape, is $(2.45 \pm 0.04 \pm 0.07) \times 10^6/\text{cm}^2/\text{s}$, and the ratio to the standard solar model of BP98 is $0.475^{+0.008}_{-0.007} \pm 0.013$.

The real time nature of the measurement makes possible to check for time variations, day/night flux differences [25], seasonal variations and other time variations. The importance of the spectrum shape measurement [26] and time variations for the study of neutrino oscillations will be discussed later.

The results from these solar neutrino experiments are listed in Table 1. Strong deficits from the predicted flux, ranging from about 30 to 60%, are observed.

4 Solar neutrino problem

How can we interpret this problem? Please notice that the suppression observed by the various experiments is not uniform, as seen in Table 1.

First suppose that neutrinos have no masses. Let us consider the results from the Cl (Homestake) and the water Cherenkov (Kamiokande/Super-Kamiokande) detectors. Super-Kamiokande measures the ^{8}B-neutrino flux and finds data/SSM$_{BP98}$= 0.475 ± 0.015 (with statistical and systematic errors combined in quadrature). Using the ^{8}B capture cross section of Chlorine, $1.14\pm0.03\times10^{-42}\text{cm}^2$ [37, 38], the chlorine experiment should observe at least $5.9\ \text{SNU}\times0.475(1\pm0.041) = 2.80\pm0.11$ SNU from the ^{8}B-neutrino contribution only. But the actual number observed is 2.56 ± 0.23. Then there could be no ^{7}Be-neutrinos observed by the Cl experiment.

Experiment	Reactions (for detection)	Threshold (MeV)	Results (Ratio to the SSM(BP98))
Homestake	$\nu_e + {}^{37}\mathrm{Cl} \rightarrow e + {}^{37}\mathrm{Ar}$	0.814	$0.332 \pm 0.021 \pm 0.021$
Kamiokande	$\nu_e + e \rightarrow \nu_e + e$	7.0	$0.544 \pm 0.037 \pm 0.064$
SAGE	$\nu_e + {}^{71}\mathrm{Ga} \rightarrow e + {}^{71}\mathrm{Ge}$	0.233	$0.517\ ^{+0.055\ +0.042}_{-0.053\ -0.044}$
GALLEX	$\nu_e + {}^{71}\mathrm{Ga} \rightarrow e + {}^{71}\mathrm{Ge}$	0.233	$0.601^{+0.059}_{-0.060}$
Super-K	$\nu_e + e \rightarrow \nu_e + e$	5.5	$0.475^{+0.008}_{-0.007} \pm 0.013$

Table 1: Recent results of the solar neutrino experiments. The ratio of the total flux measurement of each experiment to the SSM of BP98 [4] is shown. All the results except for Super-Kamiokande are those reported at the NEUTRINO'98 conference. The Super-Kamiokande result shown in this table is based on 825 days of data.

The solar luminosity constraint implies that the most of the pp-neutrino flux should be present. For the Gallium experiment, this luminosity constraint and the additional contributions from the ^{8}B-neutrinos (measured by Super-K) indicate again that there is no room for ^{7}Be-neutrinos in the gallium results.

Those two facts, with very minimal assumptions on the model of solar neutrinos, suggest that, if neutrinos have no mass, the flux of ^7Be-neutrino must be zero. But this situation is very difficult to because, since both ^{7}Be- and ^{8}B-neutrinos are produced by interactions on ^{7}Be in the sun (see Fig. 1).

Similar conclusions are obtained by more sophisticated arguments [39]. In these papers, all of the solar models are excluded at the 99% C.L.

The most natural interpretation of the data is neutrino oscillation. We should note that the strong ^{7}Be-deficit is a conclusion from the assumption that the neutrino mass is zero and there are no oscillations. Once we assume that neutrino oscillations take place, then the strong ^{7}Be-deficit may not be necessary. Other effects such as a strong deficit of pp-neutrinos can also explain the experimental situation while keeping a modest ^{7}Be-neutrino flux. To be more explicit, the assumption of a small mixing angle predicts a strong ^{7}Be-deficit with no suppression of the pp-neutrinos, while a large mixing angle solution can suppress both pp- and ^{7}Be-neutrino roughly by 50%. This will be explained in the following sections.

5 Neutrino oscillation

Neutrino oscillations [40] provide the most elegant solution of the solar neutrino problem. After the discovery of the neutrino oscillation in atmospheric neutri-

nos [1], there is almost no doubt about the solar neutrino oscillation. But, we still need to find definitive or conclusive evidence, in particular, evidence independent of the solar fluxes and an unique determination of the oscillation parameters.

For the case of two neutrinos, the transition probability for neutrinos at a distance L (km) from the source is written as

$$P(\nu_\alpha \to \nu_\beta) = \sin^2 2\theta \sin^2 \left(1.27 \cdot \Delta m^2 \cdot L/E\right) \ ,$$

where E (GeV) is the energy of neutrino and Δm^2(eV^2) is the squared mass difference of the neutrino mass eigenstates. The distance L and the energy E are determined by the experimental arrangement. If $\Delta m^2 \gg E/L$, then $P(\nu_\alpha \to \nu_\beta)$ becomes $\sim \frac{1}{2} sin^2 2\theta$. If $\Delta m^2 \ll E/L$, experiments hardly see the oscillation effect and are only able to set an upper limit $\sin 2\theta \cdot \Delta m^2 \ll 0.8[E/L]\sqrt{P(\nu_\alpha \to \nu_\beta)}$. If $\Delta m^2 \sim E/L$, experiments are maximally sensitive and we are also able to observe distance- and energy-dependent phenomena. For $E \sim 10$ MeV and $L \sim 150,000,000$ km (the solar neutrino case), the values of Δm^2 accessible by this criterion cover the range $\Delta m^2 \sim 10^{-11} \sim 10^{-10}$ eV^2.

However, there is a problem with the vacuum oscillation solution to the solar neutrino problem. Because the suppression of the flux is not uniform, a large Δm^2 cannot explain the experimental results. The value of Δm^2 must be close to E/L—the so-called Just-So oscillation [41]. Then the solutions should be around $10^{-11} \sim 10^{-10}$ eV^2.

5.1 Matter effect

When neutrinos pass through a medium, the electron neutrinos obtain an additional potential, $\sqrt{2}G_F n_e$, through the charged current forward scattering amplitude [42]. (Here G_F is the Fermi coupling constant and n_e is the number density of electrons.) The equation of neutrino propagation for the case of $\nu_e \to \nu_\mu$ is then

$$i\frac{d}{dt}\begin{pmatrix} \nu_e \\ \nu_\mu \end{pmatrix} = \begin{pmatrix} -\Delta m^2 \cos 2\theta/4p + \sqrt{2}G_F n_e & \Delta m^2 \sin 2\theta/4p \\ \Delta m^2 \sin 2\theta/4p & \Delta m^2 \sin 2\theta/4p \end{pmatrix}\begin{pmatrix} \nu_e \\ \nu_\mu \end{pmatrix} \ ,$$

where p is the neutrino momentum. The mixing angle in matter becomes

$$\tan 2\theta_m = \frac{\tan 2\theta_V}{1 - (2p\sqrt{2}G_F n_e)/\Delta m^2 \cos 2\theta_V}.$$

If $(2p\sqrt{2}G_F n_e)/(\Delta m^2 \cos 2\theta_V) = 1$ (resonance condition), then the mixing angle in matter becomes maximal, even though the vacuum mixing angle is small. If the neutrino propagates adiabatically through the resonance region, an electron

neutrino fully converts to the other flavor, ν_μ. Neutrinos of 10 MeV produced in the sun's core satisfy the resonance condition when they pass through the sun if

$$\Delta m^2 \leq 1.6 \times 10^{-4} \mathrm{eV}^2.$$

The adiabatic condition for 10 MeV neutrinos is,

$$\Delta m^2 \frac{\sin^2 2\theta}{\cos 2\theta} \geq 6.3 \times 10^{-8} \mathrm{eV}^2.$$

These conditions determine the parameter region which can potentially explain the observed conversion rate.

The matter effect also takes place when the neutrinos pass through the earth. This effect converts the ν_μ back to ν_e. The solar neutrino flux at night would, for most cases, become larger than the day flux, and therefore a so-called day/night effect would be expected.

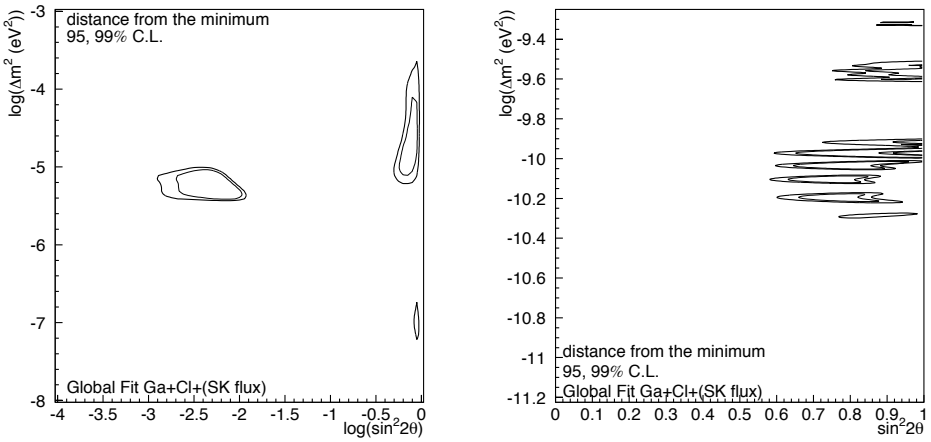

Figure 2: The oscillation parameter regions allowed at the 95% and 99% C.L. by all solar neutrino experiments. Only the total flux measurements of each experiment are used.

6 Oscillation analysis by the total flux measurement

The results of the total flux measurements by the solar neutrino experiments can be used to obtain possible neutrino oscillation parameters. Four possible

solution regions are obtained, As shown in Fig. 2, there are four possible types of solutions, characterized by their different Δm^2 and mixing angles: the MSW small mixing angle solutions ($\Delta m^2 \sim$ a few $\times 10^{-6}\mathrm{eV}^2$, $10^{-3} < \sin^2 2\theta < 10^{-2}$), the MSW large mixing angle solutions ($10^{-5} < \Delta m^2 < 10^{-4}\mathrm{eV}^2$, θ large), the LOW solutions ($\Delta m^2 \sim 10^{-7}\mathrm{eV}^2$, θ large) and the vacuum oscillation solutions (a few $\times 10^{-11} < \Delta m^2 <$ a few $\times 10^{-10}\mathrm{eV}^2$).

The small mixing angle solutions are very attractive, because we get small mixing angles in vacuum while the total oscillation probability is very large. This was one of the features that attracted people to this solution. But we now know that the atmospheric neutrino oscillation requires a large mixing. Therefore, it is equally important to explore all of the possible solutions for solar neutrino oscillations.

The results for the neutrino oscillation solutions from the total fluxes do depend on the correctness of the systematic errors of all experiments and on the solar neutrino flux calculations.

Although the flux deficits are very strong and the oscillation interpretation works very well over other explanations, the solar neutrino oscillations are not commonly thought od as an “established” result. We should note the following things:

1) When we use the total flux measurement for the oscillation analysis, we have to combine all of the experimental results. The treatment of the experimental systematic errors is difficult. We usually combine systematic errors in quadrature and treat them like statistical errors, but we do not know the probability distribution of the systematic errors. Therefore we may sometimes underestimate the systematic errors when we treat different experiments on the same footing.

2) The flux calculations may not be completely satisfactory because of the uncertainty of the nuclear cross sections, especially for the high-energy neutrinos. This is true even though the recent development of helioseismology has proved that the SSM is almost correct, and that the SSM predicts that the systematic errors are 1% for pp-neutrinos, 7% for ^{7}Be-neutrinos, and $^{+19}_{-14}$% for ^{8}B-neutrinos.

3) The possible solutions are not unique. As we have seen, there are typically four solutions.

We have two possible ways to improve this situation. The first method is to consider the flux independent measurements (at Super-K and SNO) which we will discuss next section. The other is to perform an experiment which is able to measure pp- and ^{7}Be-neutrinos separately; Borexino and LENS can do this in the future. Without these measurements, we will not be able to reach a unique solution, even though we will obtain more precise total flux data.

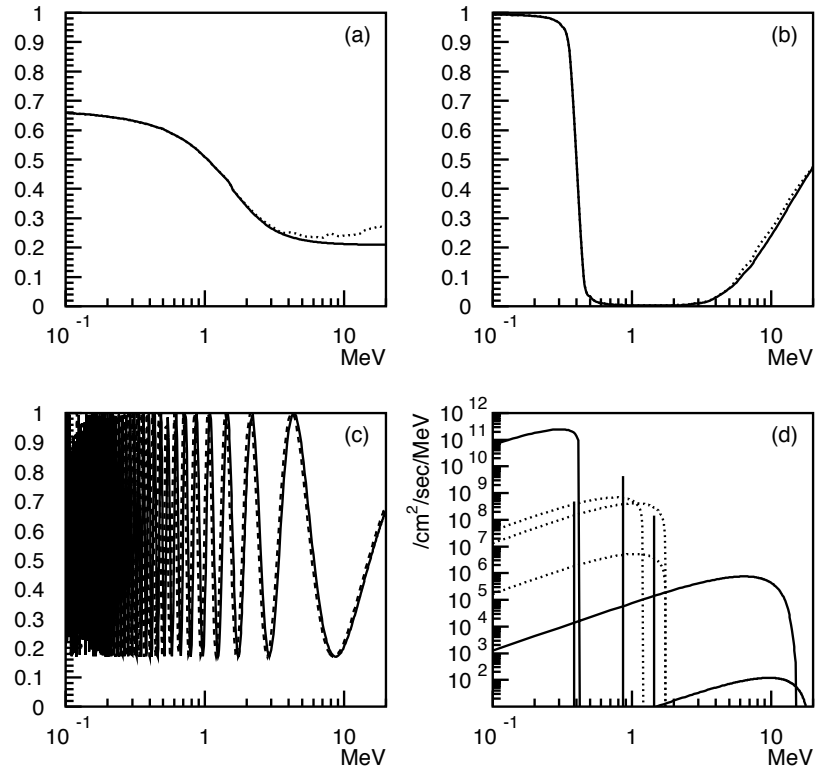

Figure 3: The distortions of the energy spectrum for different choices of oscillation parameters: (a) a large mixing angle solutions (the solid line shows the day spectrum and the dashed line shows the night spectrum), (b) a small mixing angle solution, and (c) a vacuum oscillation solution. The absolute solar neutrino spectrum is shown in (d).

7 Flux independent measurements to untangle the oscillation solutions

The model independent measurements will provide: 1) definite evidence and 2) an unique solution for the solar neutrino oscillations.

Typical examples of the energy spectrum measurements are shown in Fig. 3. For the large mixing angle solutions, we expect a day/night flux difference due to the matter effect on neutrinos passing through the earth. For the small mixing angle solutions, we expect distortions of the energy spectrum. For the vacuum solutions, we expect either spectrum distortions or seasonal variations. The LOW solutions are similar to large mixing angle solutions, but the day/night effect is expected to be larger at low energy and a smaller energy distortion is expected on the high-energy side.

Another very important measurement is the neutral current measurement, unique to SNO. This measurement can give definitive evidence of the neutrino oscillation, though it does not single out a unique solution.

To do these measurements, we need an experiment acquiring very high statistics. Currently, the necessary information only comes from Super-Kamiokande. In the very near future, SNO and Borexino will also provide flux independent measurements.

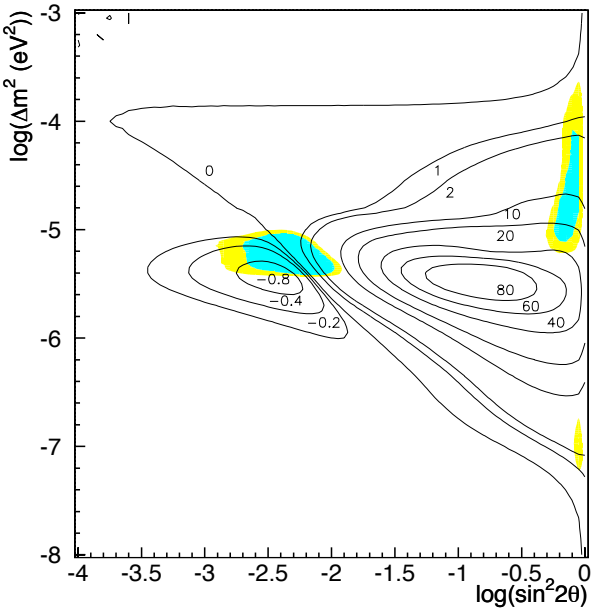

Figure 4: The expected day/night flux asymmetry. In this calculation the earth's density profile from [43] is used. The large mixing angle solutions may show a 1 to 10–20% effect. The small mixing angle solutions may have a few % effect at most.

7.1 Day/night flux difference

The day/night effect is caused by the regeneration of ν_e by the earth's matter. The difference of the densities in the sun and in the earth easily gives to the parameter region where the largest effect takes place—$\Delta m^2 \sim$ of a few $\times 10^{-6}\mathrm{eV}^2$.

Figure 4 shows the contour lines for the strength of the effect. We expect a 1% to 10 $\sim$ 20% effect for the large mixing angle solutions and a few % for LOW, whereas a few percent at most are expected for the small mixing angle solutions.

Note, however, that for some part of the small mixing angle solutions, the day/night effects are enhanced by the earth's core. The effect is very beautifully

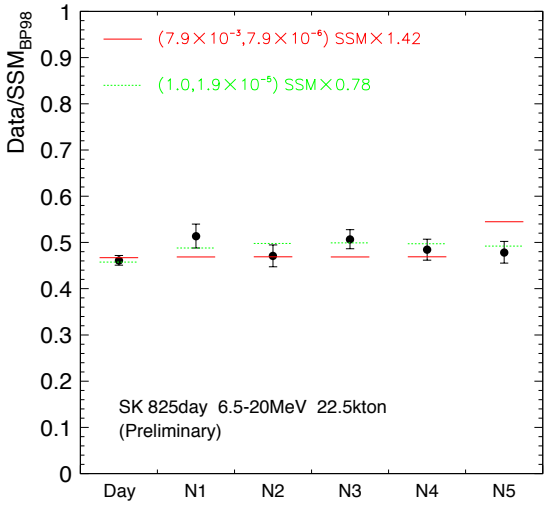

Figure 5: The observed flux of daytime and nighttime. The nighttime data are subdivided into 5 nadir angle bins with $\Delta\cos\theta_n$=0.2. Also shown are the predicted fluxes for typical oscillation parameters. The solid line and the dashed line show the flux for ($\Delta m^2 = 7.9\times10^{-6}eV^2, \sin^2 2\theta = 7.9\times10^{-3}$) and ($\Delta m^2 = 1.9\times10^{-5}eV^2, \sin^2 2\theta = 1.0$), respectively.

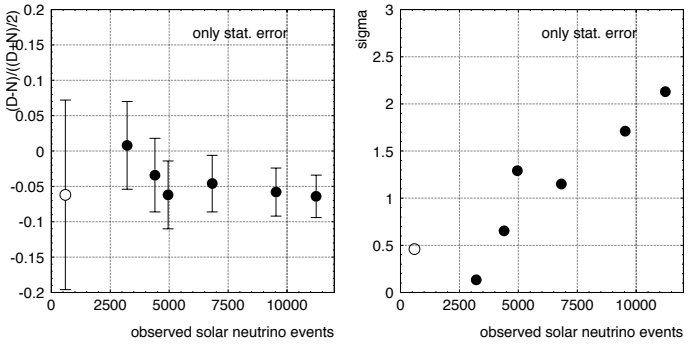

Figure 6: The development of the significance of the day/night effect observed by Super-Kamiokande as a function of time.

explained by the so-called parametric resonance [44].

The only result on the separately measured daytime and nighttime flux is that obtained by the Super-Kamiokande experiment. The day flux and the night flux are separately measured, based on 5317^{+123}_{-116} and 5905^{+131}_{-120} events, respectively, accumulated in the effective 403.2 and 421.5 days of daytime and nighttime data. The ratio obtained is $2(N-D)/(N+D) = 0.065 \pm 0.031(\text{stat.}) \pm 0.013(\text{syst.})$.

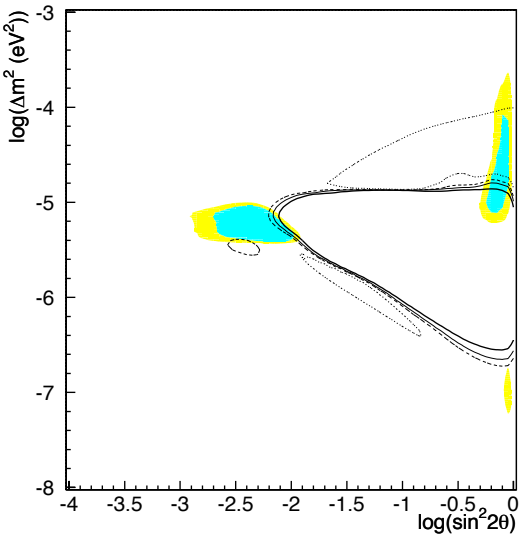

Figure 7: The confidence level regions obtained by the Super-K day/night flux difference. The thick solid line shows the 99% C.L. and the dotted line shows the 68% C.L. The other lines are 90 and 95%, respectively.

The statistical significance of this difference is 2σ. Most of the systematic error comes from the up-down asymmetry of the energy scale uncertainty, which contributes about $^{+1.2}_{-1.1}$% to the ratio; the rest of the errors are small. The nighttime data is shown in Fig. 5 in 5 bins with $\Delta\cos\theta_{zenith}$=0.2, together with expected values for some oscillation parameters. We should point out that there is no core effect seen in the data of the bin N5. If we restrict the data only to that passing through the core, corresponding to $\cos\theta_N > 0.838$, then we obtain the ratio, data/SSM=$0.451^{+0.026}_{-0.025}$ for the core data. Again, we do not see any effect within the experimental errors. This measurement actually has excluded some regions of the small mixing angle solution.

The time dependence of the significance is plotted in Fig. 6. We may define a χ^2 to evaluate the oscillation parameters. Figure 7 shows the contours corresponding 68, 90, 95, and 99% C.L. The region inside the contours of 99, 95, and 90% C.L. are excluded.

7.2 Spectrum measurement

Super-Kamiokande and SNO can measure the solar neutrino spectrum. Super-Kamiokande measures the recoil electron spectrum, which is a convolution of the solar neutrino spectrum and the differential cross section for the ν_e+e$^-$ → ν_e+e$^-$

interaction:

$$\frac{d\sigma}{dE_e} = \frac{2G_F^2}{\pi}[(g_L+1)^2 + g_R^2(1-\frac{E_e'}{E_\nu})^2 + (g_L+1)g_R\frac{m_e}{E_\nu}\frac{E_e'}{E_\nu}].$$

SNO can measure the electron spectrum from the ν_e+d→p+p+e$^-$ interaction.

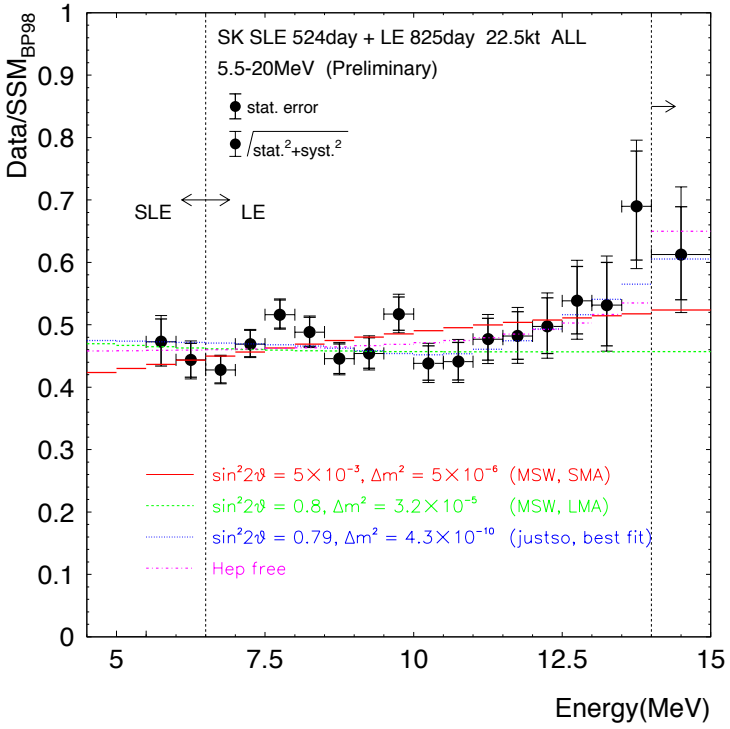

Figure 8: The recoil electron spectrum measured by Super-Kamiokande. The ratio of the data to the prediction of the SSM of BP98 is plotted. The expected ratios for typical oscillation parameters are also shown.

Currently only the data from Super-Kamiokande is available. This is shown in Fig. 8, together with the expectations for some sets of neutrino oscillation parameters.

The spectrum is sensitive to the accuracy of the energy calibration (the absolute energy scale and the energy resolution). Super-Kamiokande uses an electron LINAC to obtain the energy scale and resolution [45]. The uncertainty of the energy scale is controlled to be less than ±1% and the resolution to be less than ±5% through out the experiment. There is a slight increase of the spectrum at

the higher end. This can only be explained by systematic effects if the energy scale is wrong by 3.6% and the resolution is wrong by 20%. This is more than a 3σ deviation and is not likely to happen.

Because of the steep energy spectrum of the solar neutrinos, the number of events observed for example between 13.5 and 14 MeV ($77.0^{+9.9}_{-9.6}$ events) is less than one order of magnitude smaller than that between 6.5 and 7 MeV ($1758.4^{+92.0}_{-85.5}$ events). Therefore, the spectrum at the high-energy end is still dominated by statistics. The χ^2 for the assumption of a flat distribution is 24.3 (17 d.o.f.) corresponding to the 11% C.L.

The rise at the highest energies might be explained by the contribution from the hep-neutrinos that are produced by the process $^3He + p \rightarrow ^4 He + e^+ + \nu_e$ [15, 16]. The SSM flux of the hep-neutrinos is 2.10×10^3/cm^2/s, about three orders of magnitude smaller than the ^{8}B flux of $5.15\times10^6(1.00^{+0.19}_{-0.14})$/cm^2/s. However, the end point energy of the hep-neutrinos (18.8 MeV) is higher than that of ^{8}B (15MeV), and therefore hep-neutrinos may effect the energy spectrum of ^{8}B at the very edge of the energy spectrum.

The contribution of the hep-neutrinos is only 3.0% above 14MeV, and 1.1% between 13 and 14 MeV for the nominal hep flux. However, there is no error estimate on the hep flux in the SSM. The SSM uses S(0)$_{hep}$=2.3 ± 10^{-20} keV-b, which is the averaged value calculated by [46]. Various estimates of S(0)$_{hep}$ are listed in Table 2, taken from [46, 16]. For more detailed discussions, see, for example, [16, 47].

S(0)$_{hep}$ (10^{-20}keV-b)	Physics	Year
630	single particle	1952
3.7	forbidden	1967
8.3	better wave function	1973
4.25	D-state + meson exchange	1983
15.3	measured $^3He(n,\gamma)^4He$	1989
57	measured $^3He(n,\gamma)^4He$ shell model	1991
1.3	destructive interference	1991
1.4–3.3	Δ-isobar current	1992

Table 2: Calculated values of S(0)$_{hep}$, from [16, 46].

If we fit the energy spectrum by letting the hep flux be a free parameter, the χ^2 for the assumption of no energy distortion becomes 19.5 / 16 dof (24.4% C.L.), with 16.7 times the SSM hep flux.

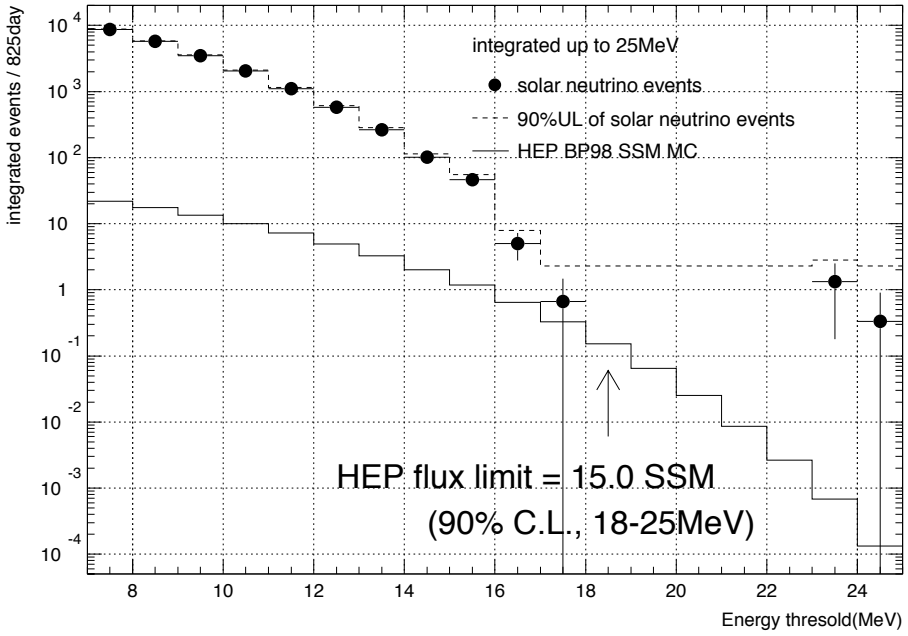

Figure 9: The high-energy solar neutrino data of Super-K. The hep flux limit is obtained from the data above 18 MeV.

The hep flux can be experimentally determined from the Super-Kamiokande data by looking at the data beyond the end point of the ^{8}B spectrum. This is shown in Fig. 9. The data above 18 MeV are used to evaluate the hep flux. Of course, one must take account of the energy spread due to the resolution. This method is, however, very difficult, because the acceptance for the hep-neutrinos is very small. The upper limit obtained is 15 times the SSM hep flux. However, considering for example, that the oscillation effect decreases the flux to $\sim$ 50%, this limit would correspond to $\sim$ 30 times SSM hep prediction.

7.3 Oscillation analysis by day/night and energy spectrum

A flux independent analysis has been performed by the Super-Kamiokande collaboration. They have used the day-spectrum and night-spectrum. Therefore they are able to include both the day/night effect and the spectrum distortion simultaneously using data sets that do not overlap. The hep-neutrinos are treated in two ways in the analysis—taking the flux to have the SSM value or to be a free

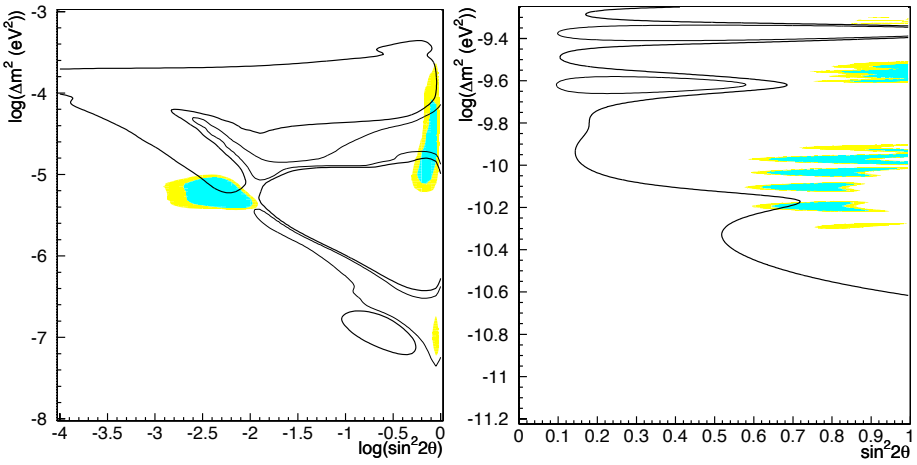

Figure 10: The confidence level contours from the Super-Kamiokande day-spectrum and night-spectrum with the SSM hep flux. The regions inside the thick solid lines are excluded at the 99% C.L. The thin solid lines show the contours of 95% C.L.

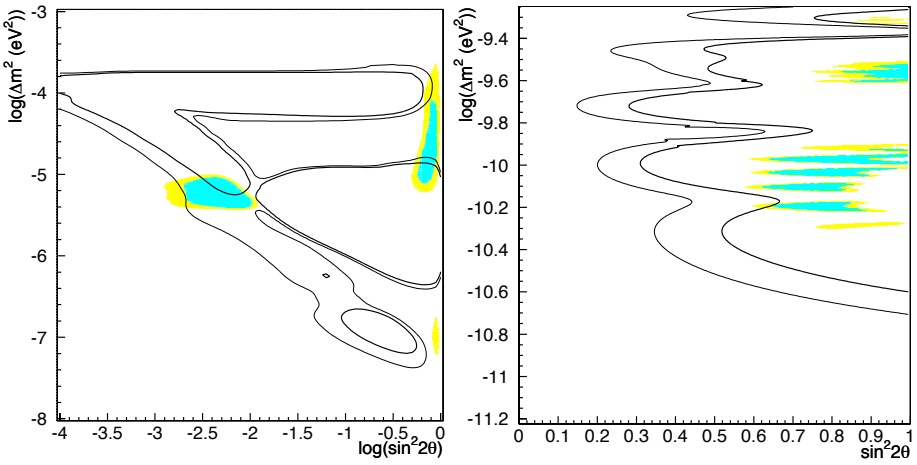

Figure 11: The confidence level contours from the Super-Kamiokande day-spectrum and night-spectrum with the hep flux as a free parameter. The regions inside the thick solid lines are excluded at the 99% C.L. The thin solid lines show the contours of 95% C.L. Due to the free hep flux, the spectrum shape loses its discrimination power and the allowed regions are extended compared to the previous figures.

parameter. The χ^2 is constructed in the following way:

$$\chi^2 = \sum_{D,N} \sum_{i=1}^{16} \{ \frac{(\frac{data}{SSM})_i - (\frac{MC_{w/oscill}}{SSM}) \alpha_{D,N} / ((1 + \delta_{i,exp} \cdot \beta)(1 + \delta_{i,cal} \cdot \gamma))}{\sigma_i} \}^2 + \beta^2 + \gamma^2,$$

where $\delta_{i,exp}$ and $\delta_{i,cal}$ are 1σ values for the correlated experimental error and for the expected spectrum calculation error as described above, σ_i is a 1σ error for each energy bin defined as a sum of statistical error and uncorrelated errors added in quadrature, and α is a free parameter which normalizes the measured flux relative to the expected flux. The parameters β and γ are used to constrain the variation of correlated systematic errors. The correlated systematic errors are treated by shifting the value in all energy bins by 0.1σ at each step. The minimum value of this χ^2 is obtained by numerically varying the oscillation parameters and the parameters α, β, and γ. This results in a minimum value of 44.1. The resulting minimum χ^2 corresponds to an agreement of the measured energy shape and the day/night flux with the expected ones at the 13.9 % confidence level.

The result of flux independent analysis with the SSM hep flux is shown in Fig. 10. The result of the flux independent analysis with hep flux left free is shown in Fig. 11.

The χ^2 values obtained for some typical oscillation parameters are show in Table 3 for the two cases. For the case with SSM hep flux, the high energy end of the spectrum has an influence on the calculation. But taking the hep flux to be free basically removes the power of the high energy data for the neutrino oscillation analysis. In this case, the day/night flux difference plays a larger role. The fact that the SMA and no oscillation hypotheses have larger χ^2 in this analysis is mainly due to the slight positive day/night effect in data.

parameters	Δm^2	$sin^2 2\theta$	χ^2 SSM hep	χ^2 hep free
LMA	3.2×10^{-5}	0.8	47.3	42.2
LOW	2.4×10^{-7}	1.0	47.5	42.0
SMA	5×10^{-6}	5×10^{-6}	53.3	51.2
VO(Large)	4.3×10^{-10}	0.79	44.1	44.2
No Oscillation			51.4	46.2

Table 3: The χ^2 values from the day/night spectrum analysis. The d.o.f. is 35 for the SSM hep analysis and 34 for hep free analysis.

The flux independent analysis has just begun to give us useful information. It gives a hint, but currently the two effects (spectrum and day/night) do not give a

stronger signature when they are combined together. For the SMA solutions, we do not expect the day/night flux difference. The day/night effect should disappear if the SMA is the correct answer. For the LMA and LOW solutions, one would expect the positive day/night effect, but no spectrum distortions. The LMA and LOW solutions may be consistent with the measurement provided that the spectrum distortion is caused by a statistical fluctuation or by the hep contribution.

If the vacuum oscillation is the correct hypothesis, one should expect seasonal variations as well as spectrum distortions, but no day/night effect. (A very small (virtual) day/night effect may be seen, which is caused by different length of the daytime and nighttime in different seasons). In any case the expected seasonal variation is very small and difficult to observe with current statistics.

The region around (4.3×10^{-10}eV^2, 0.79) which the SK data favors, has a small contradiction with the results from the analysis using only the total flux measurements. The ^{8}B flux should be reduced by 20% (1σ) in order to be consistent with the results of the model independent analysis.

If both the day/night effect and the spectrum distortion disappear, then the true solution may most probably be either 'very small' mixing angle solutions, which can be tested only by the individual determination of the pp- and ^{7}Be-neutrino flux, or the higher Δm^2 region of the large mixing angle solutions, which can be tested by the KamLAND experiment we will discuss later.

8 Global analysis

We expect that the solar neutrino problem will eventually be resolved by model independent analyses in the very near future. The current results are statistically not sufficient to make an definitive conclusion. Therefore, the Super-Kamiokande collaboration has performed a global analysis which uses all the available data. They limit their consideration to the two neutrino oscillation case; see, for example [48] for an analysis for the three neutrino case.

In this analysis they treat all of the systematic errors of each experiment and of the flux calculations as 1σ errors. Correlations of the errors, including the correlated errors of the standard solar model, are taken into account. The systematic errors among different experiments are treated as independent.

The data sets used are the total flux measurements of Homestake, SAGE, GALLEX, Kamioka, and the day/night spectrum data from Super-Kamiokande with flux constraint. The prescription they have adopted is similar to [49] and references therein. A similar analysis has recently done also by [50].

Two analyses were conducted as in the model independent analyses in previous section: one with the standard hep-neutrino flux and the other considering the hep-neutrino as a free parameter. The results are shown in Figs. 12 and 13

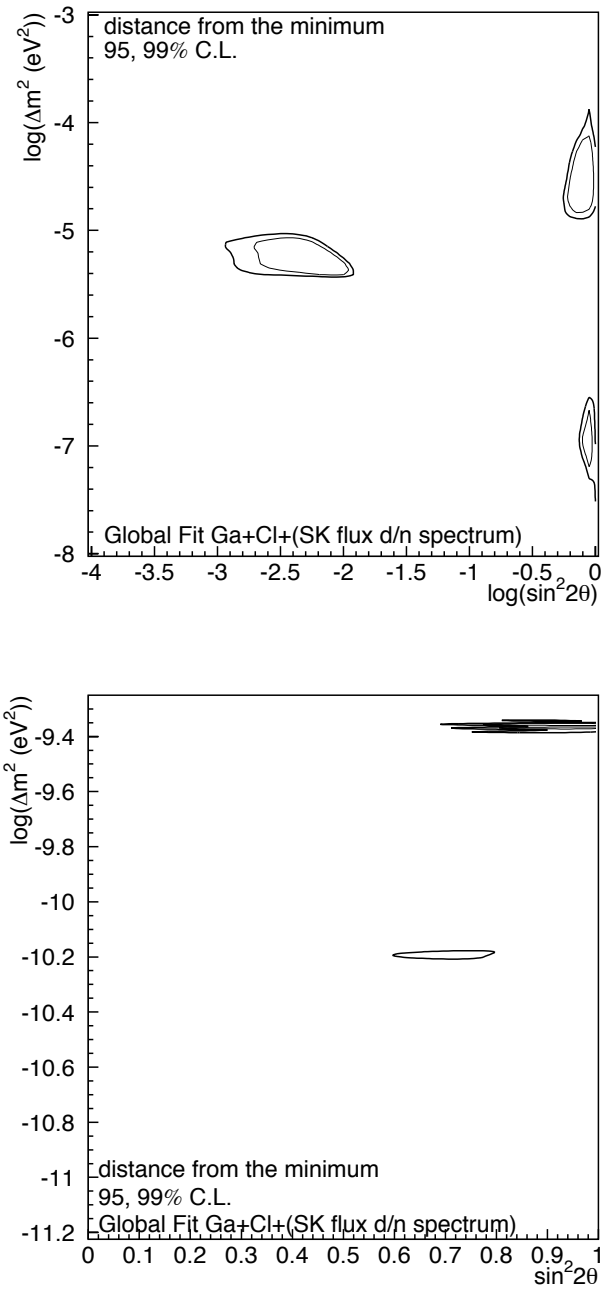

Figure 12: The results of the SK global analysis with the SSM hep flux. The 99% and 95% C.L. allowed regions are shown.

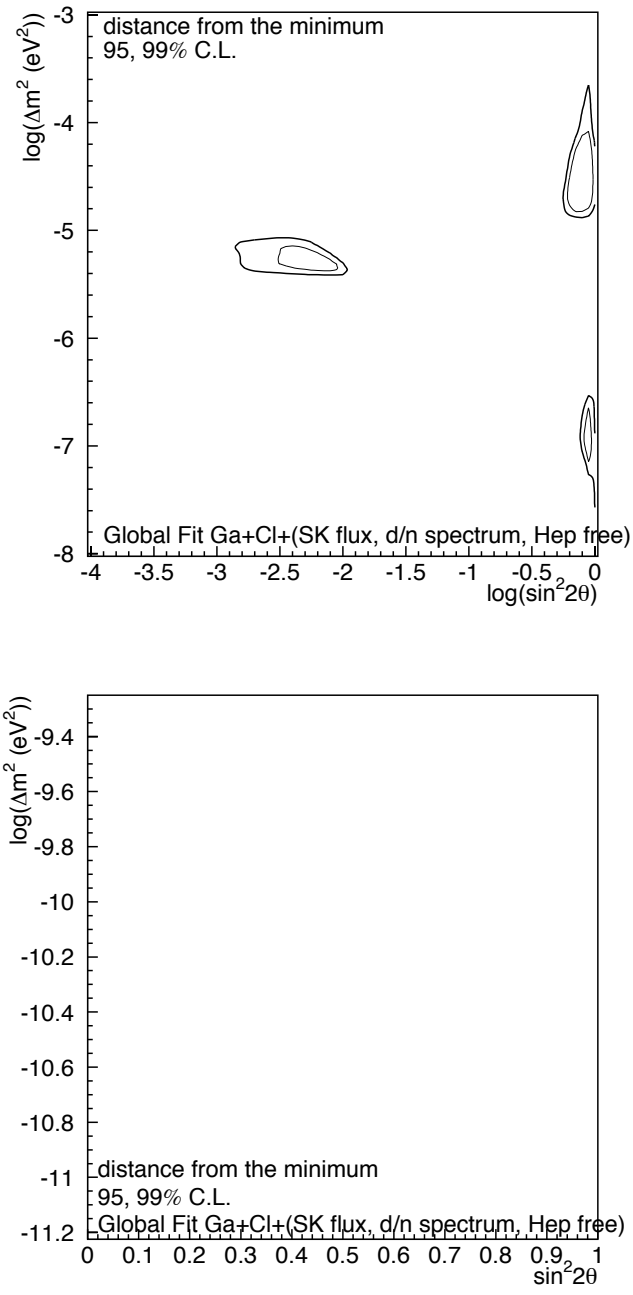

Figure 13: The results of the SK global analysis with the hep flux as a free parameter. The 99% and 95% C.L. allowed regions are shown

as 95% and 99% C.L. allowed parameter regions.

The vacuum region becomes insignificant in the global analysis because the vacuum regions favored by the total flux measurements and by the SK spectrum 'distortion' disagree with one another. In the hep free analysis, the vacuum region actually disappears. But, one must remember that the hep free analysis effectively does not use (throws away) the high-energy part of the spectrum where the signature of the vacuum oscillation shows up. Therefore, we should not take this conclusion too seriously until we will obtain a reasonable estimate of the uncertainty of the hep flux.

9 Future of solar neutrino experiments

9.1 Super-Kamiokande

Super-Kamiokande will lower its energy threshold to 4.5–5.0 MeV in the year 2000. The lower threshold increases the ability to discriminate the oscillation solutions, as seen in Fig. 8, and also increases the statistical significance. The collaboration is making further efforts to reduce the low energy backgrounds by reducing the Rn in water and the γ-ray backgrounds from the wall. This will be accomplished by improving the water circulation system and upgrading the analysis software. Another effort to reduce backgrounds even in the high-energy region invovles further reducing the spallation backgrounds and better separating γ's from electrons. All these efforts will improve the statistical significance of the data.

9.2 SNO

SNO [27, 28, 51] uses 1,000 tons of D_2O as a target material. The detector is placed 2,000 m under ground, where the penetrating cosmic ray background is reduced to a few events per day, giving small spallation backgrounds in the data. The charged current interaction is measured through the reaction, ν_e+d $\rightarrow$ p+p+e$^-$ ($Q = -1.44$ MeV). The expected event rate is about 9 per day for the flux of 0.5$\times$SSM. SNO can also measure the neutral current interaction separately through,

$$\nu_x + d \rightarrow p + n + \nu_x \qquad (Q = -2.2 \text{ MeV}) \ ,$$

with the expected number of about 3 events per day. In addition, SNO can detect neutrino elastic scattering on electrons, which yields about 1 event per day.

The flux ratio of the charged current interaction to the neutral current interaction will give definitive demonstration of neutrino oscillations. In order to

determine the oscillation parameters uniquely, SNO would also need to utilize the measurement of the energy spectrum and the day/night effect.

SNO has begun its run in May 1999 and is currently (as of the end of year 1999) doing calibrations and taking data. We expect the first news from SNO in the very near future, possibly at summer conferences in 2000.

9.3 Borexino

Borexino [52, 53] aims to measure the solar neutrino spectrum above 250 keV with 100 fiducial tons of liquid scintillator through ν_e+e $\rightarrow$ ν_e+e interactions. It is mostly sensitive to the ^{7}Be-solar neutrinos. One expects 55 events/day for the standard solar model prediction.

For the small mixing angle solutions, the ^{7}Be-solar neutrinos are almost fully depleted and only the neutral current interactions of neutrinos would be detected; this would give only 12 events/day. For the LMA solution, Borexino would detect about half of the expected flux. A distinct seasonal variation is expected for a vacuum oscillation solution, and this can be determined independently of the knowledge of the absolute flux.

The challenge of the experiment is the requirement that the U/Th contamination in the detector must be less than 10^{-15}g/g. A test facility has been set up and various studies have been performed. The experiment is expected to start operation in 2001.

9.4 KamLAND

KamLAND [54] is not a solar neutrino experiment but, rather, a long baseline reactor experiment. However, this experiment is sensitive to the MSW large mixing angle region, down to $\Delta m^2 > 10^{-5}$eV^2. The typical distance to the nuclear power reactors ($\sim$ 150 km) and the averaged anti-neutrino energy ($\sim$ 5 MeV) gives $E/L \sim 3 \times 10^{-5}$eV^2. The expected event rate is 700 events/kt/year. This experiment is hosted by Tohoku University Japan. It is a conversion of the old KAMIOKANDE detector, using a spherical stainless steel container holding 1,200m^3 liquid scintillator, which is viewed by 1,280 17-inch PMTs covering 20% of the inner surface. The container is surrounded by 3,000 tons of pure water to provide active shielding.

The experiment is fully funded and expected to start in April 2001.

10 Conclusions

The solar neutrino experiments have revealed strong flux deficits that suggest the presence of neutrino oscillations. Four distinct possible parameter regions—the MSW small mixing angle, the MSW large mixing angle, the so called LOW, and the vacuum solutions—are inferred from the results of those experiments.

The flux independent evidence, including spectrum distortions, daytime/nighttime flux differences, and seasonal variations, will provide definitive and conclusive proof of the solar neutrino oscillation, and will possibly also determines unique oscillation parameters. Those measurements have just begun, and we expect to obtain important information in very near future.

In the global analysis that treats the hep flux as a free parameter, the vacuum solutions seem to be disfavored. However, it is too early to conclude that the vacuum solution is excluded, as we have explained in a previous session.

In the future, two different directions are equally important.

First, the model independent analysis will be continued with much higher statistical sensitivities. Super-K and SNO will certainly provide interesting results in the next few years. If the large mixing angle solution is the right one, Super-Kamiokande will observe a positive day/night effect. Later, KamLAND should confirm this result by the measurement of neutrino oscillations from nuclear reactor sources. SNO will give definitive evidence of neutrino oscillations through the separate measurement of neutral and charged current interactions. But this neutral current itself cannot discriminate the possible solutions. SNO may also have a better energy response than that in Super-K and would, therefore, eventually provide a better demonstration of the energy distortion characteristic of the MSW SMA solutions.

Another direction that will be pursued is to measure separately the pp- and ^{7}Be-neutrino fluxes. The current experiments cannot discriminate the pp- and ^{7}Be-neutrino events, and thus it is impossible to determine which part of the spectrum is missing. A separate determination of the low energy solar neutrinos from these sources would be a big step towards discriminating the solutions. Borexino aims to measure the ^{7}Be-neutrino flux. This experiment could also make a good test of the vacuum oscillation solution by looking for seasonal variations.

At the same time, Homestake, SNO/GALLEX, and SAGE will keep providing precise results. New types of detectors such as HELLAZ and LENZ will, in the future, give us the flux and the spectrum of the pp-neutrinos.

Unfortunately, we are not able to make a definitive statement on solar neutrinos at this time. However, new experimental results will provide a definitive answer. The resolution of the solar neutrino problem is one of the most important issues for the next few years in understanding the mixing and mass matrix of neutrinos. Neutrino oscillations give a clue to the physics beyond the standard

model of elementary particle physics. They will guide us to the world of the huge energy scales that stand behind the tiny values of the neutrino masses.

References

[1] Y. Fukuda *et al.*, Phys. Rev. Lett. **81**, 1562 (1998).

[2] J. N. Bahcall and R. Davis, Jr., astro-ph/9911486.

[3] K. S. Hirata *et al.*, Phys. Lett. **B205**, 416(1988).

[4] J. N. Bahcall, S. Basu and M. Pinsonneault, astro-ph/9805135.

[5] A. S. Brun, S. Turck-Chieze and P. Morel, Ap. J. **506**, 913 (1998).

[6] E. G. Adelberger *et al.*, Rev. Mod. Phys. **70**, 1265 (1998).

[7] C. A. Iglesias and F. J. Rogers, Astrophys. J. **464**, 943 (1996).

[8] F. J. Rogers, F. J. Swenson and C. A. Iglesias, Astrophys. J. **456**, 902 (1996).

[9] A. V. Gruzinov and J. N. Bahcall, Astrophys, J. (in press), astro-ph/9801028.

[10] J. N. Bahcall and M. Pinsonneault, Rev. Mod. Phys. **67**, 781 (1995).

[11] J. N. Bahcall, Neutrino Astrophysics. (Cambridge University Press, 1989).

[12] J. N. Bahcall and P. I. Krastev, Phys. Rev. **D53**, No.8, 4211 (1996).

[13] S. Degl'Innocenti, W. A. Dziembowski, G. Fiorentini, B. Ricci, Astroparticle Physics **7**, 77 (1997).

[14] J. N. Bahcall, M. H. Pinsonneault, S. Basu and J. Christensen-Dalasgaard, Phys. Rev. Lett. **78**, 171 (1997).

[15] R. Escribano, J.-M. Frere, A. Gevaert, and D. Nonderen, Phys. Lett. **B444**, 397 (1998).

[16] J. N. Bahcall and P. I. Krastev, Phys. Lett. **B436**, 243 (1988).

[17] J. N. Bahcall and A.Ulmer, Phys. Rev. **D53**, 4202 (1996).

[18] B. T. Cleveland *et al.*, Ap. J. **496**, 505 (1998), B. T. Cleveland *et al.*, Nucl. Phys. B(Proc. Suppl.) **38**, 47 (1995); R. Davis, Prog. Part. Nucl. Phys. **32**, 13 (1994).

[19] K. S. Hirata *et al.*, Phys. Rev. Lett. **65**, 1297 (1990); K. S. Hirata *et al.*, Phys. Rev. **D44**, 2241 (1991); **D45**, 2170E (1992).

[20] K. S. Hirata *et al.*, Phys. Rev. Lett. **66**, 9 (1991).

[21] Y. Fukuda *et al.*, Phys. Rev. Lett. **77**, 1683 (1996).

[22] J. N. Abdurashitov *et al.*, Phys. Lett. **B328**, 234 (1994).

[23] P. Anselmann *et al.*, Phys. Lett. **B285**, 376 (1992); W. Hampel *et al.*, Phys. Lett. **B388**, 364 (1996).

[24] Y. Fukuda *et al.*, Phys. Rev. Lett. **81**, 1158 (1998).

[25] Y. Fukuda *et al.*, Phys. Rev. Lett. **82**, 1810 (1999).

[26] Y. Fukuda *et al.*, Phys. Rev. Lett. **82**, 2430 (1999).

[27] H. H. Chen, Phys. Rev. Lett. **55**, 1534 (1985).

[28] G. T. Ewan *et al.*, Sudbury Neutrino Observatory Proposal - SNO 87-12(1987).

[29] K. Lande, in Neutrino '98, Proceedings of XVIII International Conference on Neutrino Physics and Astrophysics (Takayama, Japan, 1998), eds. Y. Suzuki and Y. Totsuka; Nucl. Phys. B(Proc. Suppl.) **77**, 13 (1999).

[30] V. N. Gavrin, in Neutrino '98; Nucl. Phys. **B** (Proc. Suppl.) **77**, 20 (1999).

[31] W. Hampel *et al.*, Phys. Lett. **B447**, 127 (1999).

[32] M. Cribier *et al.*, Nucl. Instr. Meth. **A378**, 233 (1996).

[33] P. Anselmann *et al.*, Phys. Lett. **B342**, 440 (1995).

[34] W. Hampel *et al.*, Phys. Lett. **B420**, 114 (1998).

[35] J. N. Abdurashitov *et al.*, Phys. ReV. C (1998) submitted.

[36] W. Hampel *et al.*, Phys. Lett. **B436**, 158 (1998).

[37] M. B. Aufderheide, S. D. Bloom, D. A. Resler, C. D. Goodman, Phys. Rev. **C49**, 678 (1994).

[38] J. N. Bahcall *et al.*, Phys. Rev. **C54**, 411 (1996).

[39] See, for example, [50] and references therein.

[40] J. Maki, M. Nakagawa, S. Sakata, Prog. Theor. Phys. **28**, 870 (1962).

[41] L. Glashow and L. M. Krauss, Phys. Lett. **B190**, 199 (1987).

[42] S. P. Mikheyev and A. Y. Smirnov, Sov. Jour. Nucl. Phys. **42**, 913 (1985); L. Wolfenstein, Phys. Rev. **D17**, 2369 (1978).

[43] A. M. Dziewonski and D. L. Anderson, Phys. Earth Planet. Inter. **25**, 297 (1981).

[44] S. T. Petcov, Phys. Lett. **B434**, 321 (1998).

[45] M. Nakahata *et al.*, Nucl. Instr. and Meth. **A421**, 113 (1999).

[46] R. Schiavilla, R. B. Wiringa, V. R. Pandhariande, J. Carlson, Phys. Rev. **C45**, 2628 (1992).

[47] G. Fiorentini, V. Berezinsky, S. Degl'Innocenti and B. Ricci, Phys. Lett. **B444**, 387 (1998).

[48] G. L. Fogli, E. Lisi, D. Montanino, and A. Palazzo, BARI-TH/365-99.

[49] G. L. Fogli and E. Lisi, Astrop. Physics. **3**, 185 (1995).

[50] J. N. Bahcall, P. I. Krastev, A. Yu. Smirnov, Phys. Rev. **D58**, 096016 (1998).

[51] A. B. McDonald, Nucl. Phys. **B** (Proc.Suppl.) **77** ,43 (1999).

[52] C. Arpesella *et al.*, Borexino proposal, Vols. 1 and 2, eds. G. Bellini, R. Raghavan *et al.*, (Univ. of Milano, Milano, 1992).

[53] L. Oberauer, Neutrino'98, Nucl. Phys. **B** (Proc. Suppl.) **77**, 48 (1999).

[54] A. Suzuki [KamLAND Collaboration], Nucl. Phys. **B** (Proc. Suppl.) **77**, 171 (1999).